Bifurcation Phenomena of a Magnetic Island at a Rational Surface in a Magnetic-Shear Control Experiment

K. Ida, S. Inagaki,* M. Yoshinuma, Y. Narushima, K. Itoh, T. Kobuchi,† K. Y. Watanabe, H. Funaba, S. Sakakibara, T. Morisaki, and LHD Experimental Group

National Institute for Fusion Sciences, Toki, Gifu 509-5292, Japan

(Received 28 June 2007; published 30 January 2008)

Three states of a magnetic island are observed when the magnetic shear at the rational surface is modified using inductive current associated with the neutral beam current drive in the Large Helical Device. One state is the healed magnetic island with a zero island width. The second state is the saturated magnetic island with partial flattening of the T_e profile. The third state is characterized by the global flattening of the T_e profile in the core region. As the plasma assumes each of the three states consecutively through a bifurcation process a clear hysteresis in the relation between the size of the magnetic island and the magnetic shear is observed.

DOI: 10.1103/PhysRevLett.100.045003 PACS numbers: 52.55.Hc, 52.30.Cv, 52.35.Vd

Studies of the neoclassical tearing mode in tokamak plasmas have been made in various experimental devices because of its importance to predict the performance of confinement [1–4], and stabilization of this mode by electron cychlotron current drive has been demonstrated in tokamaks [5–7]. Although the influence of magnetic shear on MHD activity is important in addition to its influence on transport, an experimental study based on the actual measured magnetic shear has not been made in a helical system. This is because the magnetic shear originally produced by the external coil currents is large enough to shrink the magnetic island even if there is some residual error magnetic field [8,9] and comparison with theoretical model was reported [10]. It has been pointed out that the global stochastization of the magnetic surfaces is induced when the width of the island exceeds a threshold in toroidal plasmas [11]. Therefore the effect of the magnetic shear on the formation of a magnetic island, on the stochastization of magnetic surfaces, and on MHD instabilities such as the tearing mode and the interchange mode [12] has been considered to be a very important issue in tokamak and stellarator plasmas. This study is very important in the plasma with a low shear configuration because the MHD activity is sensitive to the magnetic shear at the rational surface. Although the plasma current in a helical system is a relatively small fraction of the equivalent plasma current, the magnetic shear near the plasma center can be controlled by driving a current at the magnetic axis. Neutral beam current drive (NBCD) is one of the useful tools to drive the toroidal current; however, the current drive by NBCD has not been studied much because of the difficulty of measurement of the pitch angle of the magnetic field in a stellarator.

The Large Helical Device (LHD) is a heliotron-type device which has three tangential neutral beams, and two beams are used to drive the plasma current in the direction parallel (coinjection) or antiparallel (counterinjection) to the equivalent plasma current, while one beam is always used as a probe beam of the motional Stark effect (MSE) spectroscopy [13]. The radial profiles of the rotational transform (ι) are derived from the polarization angle measured with MSE spectroscopy using an equilibrium code. The electron temperature (T_e) is measured with an electron cyclotron emission (ECE) radiometer [14]. In this experiment the magnetic field, B, is 2.75 T, and the major and minor radius of the plasma R and a is 3.6 m and 0.6 m, respectively, where the magnetic shear is negative (standard stellarator shear) with a magnetic hill configuration. The direction of the neutral beam is switched at the middle of the discharge with a relatively low density of 1×10^{19} m^{-3}.

Figures 1(a) and 1(b) show the time evolution of ι at various radii and total plasma current. The direction of the injected neutral beam switches from parallel (codirection)

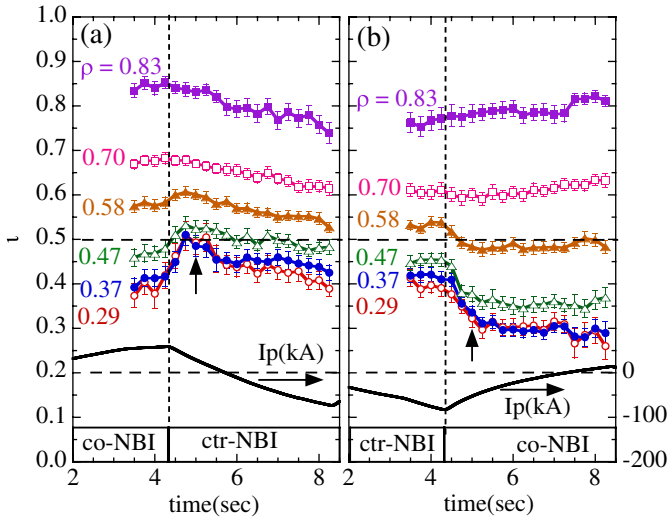

FIG. 1 (color online). Time evolution of rotational transform (ι) at various plasma radii and total plasma current in the plasma with the neutral beam injection (a) from coinjection to counterinjection and (b) from the counterinjection to coinjection.

to antiparallel (counterdirection) to the equivalent plasma current or vice versa at $t = 4.3$ sec. Although the change in ι near the plasma edge ($\rho = 0.83$) is due to the neutral beam current drive and consistent with that of total plasma current, the change in rotational transform at the plasma core region ($\rho < 0.5$) is opposite to that at the plasma edge. The total plasma current driven by the neutral beam is in the range of -100 kA (counterdirection) to 50 kA (co-direction), which is only 3%–6% of equivalent plasma current (1.8 MA) produced by the external helical coils. The change in ι in the core region is due to the inductive current compensating the toroidal current driven by the neutral beam. Although the time scale in the change of total current is longer than the beam pulse (4 sec each), the time scale of the change in ι and the magnetic shear due to the inductive current is only a half second. It should be noted that the ι and magnetic shear in the plasma core at $t = 5.5$ sec in the discharge with coinjection (co) to counterinjection (ctr) [in Fig. 1(b)] and $t = 7.5$ sec in the discharge with ctr to co [in Fig. 1(a)] are quite different, although the total plasma current is zero for both discharges. This experiment demonstrates that the toroidal current driven by the neutral beam has a significant effect on the magnetic shear because of the inductive current associated with the injection of the neutral beam.

As seen in Fig. 2, the ι in the core region increases and reaches up to 0.5 and the magnetic shear in the core region ($\rho < 0.4$) becomes close to zero after the switching of the beam from co to ctr. In contrast, the radial profile of the ι in the discharge where the beam switches from ctr to co has strong magnetic shear at the rational surface of $\iota = 0.5$ because the central ι drops after the switch of the beam from ctr to co. A flattening of T_e is observed when the magnetic shear at the rational surface is small as seen in Fig. 2. In general, heat transport inside a magnetic island with nested magnetic flux surfaces is significantly reduced to a level much smaller than that outside the magnetic island. The flattening of T_e inside the $m = 1$ magnetic island with nested magnetic flux surfaces is due to the lack of heating power not due to the increase of heat diffusivity [15]. However, in this experiment, there is a significant fraction of the heat deposition power (32% of the total deposition power) inside the flattened region ($\rho < 0.4$). The effective thermal diffusivity, simply evaluated from the power balance at $\rho = 0.3 \pm 0.1$, $\chi_e > 10^2$ m^2/s for the discharge with co to ctr and 3 m^2/s for the discharge with ctr to co. Therefore the flattening of T_e is not due to the lack of heating power but due to the stochastic magnetic island at $\iota = 0.5$ [11].

Figure 3 shows the time evolution of the T_e gradient and magnetic shear at $\iota = 0.5$ averaged over $\Delta\rho = \pm 0.1$ for the discharge with co to ctr and ctr and co. In the discharge with co to ctr, the magnetic shear decreases gradually from 0.8 to 0 after the switch of the beam at $t = 4.3$ sec because the ι near the edge decreases due to the toroidal current driven by the neutral beam and because the rotational transform near the core increases due to the inductive current. Although the change in magnetic shear is gradual, the change in the T_e gradient is abrupt. (The jump of $\partial T_e/\partial\rho$ is faster than 0.25 sec, which is the time resolution of MSE measurements.) The T_e gradient suddenly decreases when the magnetic shear decreases below 0.15 without significant fluctuations in T_e measured with ECE. The flattening of T_e profiles extends up to 0.46 as

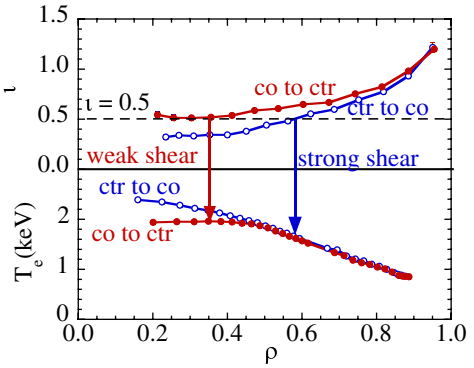

FIG. 2 (color online). Radial profile of rotational transform (ι) and electron temperature in the plasma with weak magnetic shear (at $t = 5$ sec in the discharge with co to ctr in Fig. 1(a)] and a strong magnetic shear (at $t = 5$ sec in the discharge with ctr to co in Fig. 1(b)].

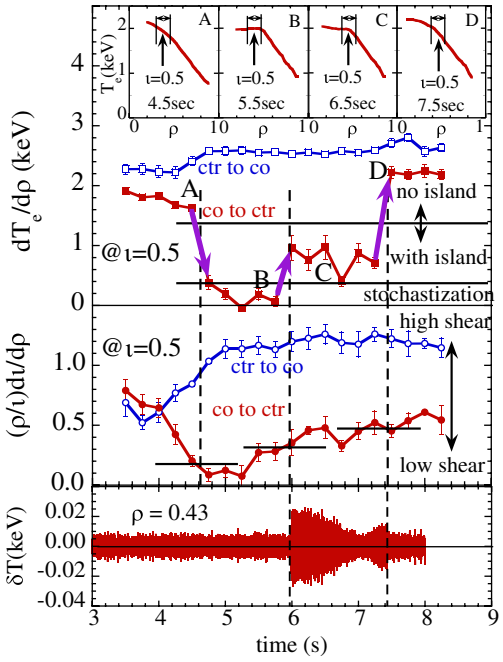

FIG. 3 (color online). Time evolution temperature gradient and magnetic shear averaged over $\Delta\rho = \pm 0.1$ at the rational surface of $\iota = 0.5$ and temperature fluctuations in the frequency range of 0.8–1.2 kHz. The radial profiles of electron temperature in the temperature flattening phase with and without MHD instability and in the peaked profile phase are also indicated.

seen in phases B and C in Fig. 3. The location of the ι of 0.5 moves outward in time and reaches to the boundary of the flattening region at $t = 6$ sec; then the MHD instability appears as seen in the fluctuation of T_e in the frequency range of 0.8–1.2 kHz. The MHD instability is localized at $\iota = 0.5$ and considered to be an interchange mode [12]. In this phase, the T_e gradient near the core ($\rho < 0.3$) recovers to the level of 0.6 keV/m ($@\rho = 0.2$), which corresponds to $\chi_e = 5$ m^2/s, but the flattening of the T_e profile still remains as seen in phase C. Associated with the disappearance of MHD fluctuations at $t = 7.4$ sec, the flattening of T_e disappears and the T_e gradient recovers to the level before the beam switch. In the discharge with ctr to co, the magnetic shear at $\iota = 0.5$ gradually increases from 0.7 to 1.2, and the magnetic shear is considered to be large enough to eliminate MHD activity. The disappearance of the pressure gradient in a wide range of radius (phase B) suggests the onset of global stochastization there. The sharp rise of the T_e fluctuation δT_e at $t = 5.985$ sec suggests a sudden recovery of the pressure gradient (within $\Delta t \leq 20$ ms) at the location where the δT_e is observed, because the pressure gradient is the necessary condition for MHD instability. The very abrupt on-and-off stochastization at the threshold is seen in the time evolution of the T_e gradient. The primary mode number of the interchange mode, m/n, is 2/1, and a low-n ideal mode calculation [16] predicts that this mode spreads in a wide region of the plasma [17] ($\rho = 0.26$–0.58) around the $\iota = 0.5$ surface. In experiments, T_e fluctuations are observed in the region of $\rho = 0.41$–0.58 with a FWHM of 0.17, which is located at a different flux surface from the 2/1 magnetic island indicated by the flat region of T_e of $\rho = 0.34$–0.43.

As seen in Fig. 4, the T_e gradient drops at the magnetic shear of 0.15, while it recovers at a relatively strong magnetic shear of 0.45. The interchange mode appears at a low magnetic field shear of 0.45 with a finite T_e gradient, of 0.5–1.0 keV, where the growth rate of low-n ideal mode γ/ω_A ($\omega_A = v_A/R$, where v_A is Alfvén velocity) at the $\iota = 0.5$ rational surface exceeds 10^{-3}. It is interesting that there is no interchange mode observed during the drop in the T_e gradient due to the magnetic island formation, although the magnetic field shear is low enough to expect the appearance of the interchange mode. When the magnetic shear is large enough (>0.5), there is no temperature flattening and the T_e gradient tends to increase as the magnetic shear is increased from 0.5 to 1.2. This dependence is considered to be due to the change in transport, which has a relatively weak dependence on magnetic shear. When the perturbation of the radial magnetic field is constant, the size of the magnetic island is expected to be proportional to the inverse of the magnetic shear. However, the magnetic island is healed at higher magnetic shear and suddenly grows as the magnetic shear drops below the critical value of 0.15. The size of the magnetic island is even larger than that expected from the error field (dotted line in Fig. 4(b), which is proportional to the inverse of the magnetic shear) because of the stochastization of the magnetic island. The growth of this stochastic magnetic island is within 50 ms without a significant fluctuation in T_e and this time scale is much shorter than the time scale of change in magnetic shear and the size of the magnetic island decreases as the magnetic shear increases. When the magnetic shear reaches 0.45, the size of the magnetic island decreases and finally disappears (magnetic island healing). The healing of the magnetic island occurs gradually in a time scale of $\Delta t = 1.2$ sec. However, the response of $\partial T/\partial \rho$ indicates that the termination of the island occurs, at the end (phase D), in a short time scale of ≤50 ms. It should be noted that interchange-type MHD fluctuations are observed during this healing phase.

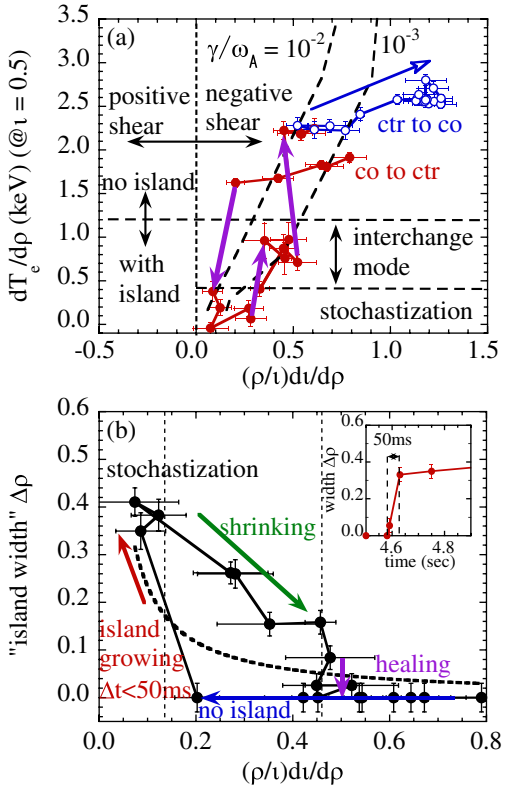

FIG. 4 (color online). (a) Electron temperature (T_e) gradient averaged over $\Delta\rho = \pm 0.1$ around the $\iota = 0.5$ rational surface and (b) size of the magnetic island as a function of magnetic shear at the $\iota = 0.5$ rational surface.

Figure 4 illuminates two characteristic features of the response of the magnetic island. First, there is hysteresis; i.e., the two states (with and without islands) are self-sustained. Second, the jump between them takes place much faster than the resistive diffusion time, which is characteristic of the change of the magnetic shear. These two essential features are understood by considering the evolution of the (stable) neoclassical tearing mode in the presence of drive by the external helical field, as is explained as follows. In the Rutherford regime of the island

evolution, the equation that describes the evolution of the resonant magnetic island is given as

$$\frac{\partial \hat{A}}{\partial t} = \frac{1}{\tau_R}\left[2|\Delta_0'|\left(\frac{\delta^2}{r_s^2}\frac{1}{\hat{A}} - 1\right)\hat{A}^{1/2} - 2\epsilon^{1/2}\beta_p a_{pc}\left(\frac{L_q}{L_p}\right)^2 \frac{(\rho_b/r_s)^2\hat{A}}{(\rho_b/r_s)^4 + \hat{A}^2}\right], \quad (1)$$

where τ_R ($= \mu_0 a^2/\eta_{NC}$) is a resistive diffusion time, ρ_b is an ion banana width, and $\hat{A}$ is a normalized amplitude of the vector potential given by $A_* q^2 R/(B r_s^3 q\prime)$, where $q(= 1/\iota)$ is the safety factor and A_* is the (m, n) Fourier component of the helical vector potential perturbation at the rational surface of r_s [18]. Here, the time and the length are normalized to a poloidal Alfvén transit time $\tau_{Ap} = qR/v_A$ (v_A: Alfvén velocity) and r_s, respectively. The first term on the right-hand side (RHS) of Eq. (1) stands for the effect of the external resonant current (Δ_0': the stabilizing influence in the absence of the external current; δ: the width of an externally driven magnetic island in a stationary state [19]). Terms due to the bootstrap current and the Glasser *et al.* effect [20] are neglected, because the influence of these terms to the peak height of $\partial\hat{A}/\partial t$ is small. The time scale of the bifurcation is mainly determined by the stabilizing influence of the ion polarization current, the second term on the RHS of Eq. (1). The coefficient a_{pc} is of the order of unity.

For the steady state solution ($\partial\hat{A}/\partial t = 0$), Eq. (1) can have 1 or 3 solutions of A, depending on the magnitude of δ/ρ_b. When the shear is strong and δ/ρ_b is small ($< O(1)$) the stabilizing effect of the polarization drift dominates the dynamics and Eq. (1) has one solution of $\hat{A}(\approx 0)$. On the other hand, when the δ/ρ_b is large, ($\delta/\rho_b \geq 5$ for present parameters) the effect of polarization drift becomes small and the magnetic island appears and Eq. (1) has another solution of $\hat{A}(\approx \delta^2/r_s^2)$. When the δ/ρ_b has an intermediate value (≤ 5), three solutions exist in the plasma. In the present experiment, the initial state is island-free ($\delta \approx 0$), and the transition takes place at $\delta/\rho_b \approx 5.3$ ($t = 4.5$ sec) in Fig. 4. Once the island is generated it is self-sustained so that the width remains finite although the shear becomes stronger. When δ/ρ_b becomes as small as ≈ 2, the back transition takes place. The other important issue is the rapidness of the jump of the width. The characteristic time scale of the transition can be derived from Eq. (1), and it is $\tau_R/(2|\Delta_0'|r_s\rho_b^{-1})$. The growth rate of the magnetic island is accelerated by $(2|\Delta_0'|r_s\rho_b^{-1}) \approx 10^2$ compared with τ_R (2–3 sec) in this experiment. In this experiment the time scale of the growth of the magnetic island is predicted to be a few tenth milliseconds and is consistent with the experimental observation. Thus, the essential hysteresis features of island evolution are qualitatively understood from the dynamics of Eq. (1).

Magnetic shear near the plasma core is controlled using inductive current associated with the neutral beam current drive in the LHD. This experiment demonstrates that the saturated magnetic island can be healed (no magnetic island) or can be stochastic (large magnetic island) depending on the magnitude of the magnetic shear. There are two bifurcation phenomena observed in this experiment. One is the bifurcation between the saturation and the healing of the magnetic island (appearance and disappearance of magnetic island), and the other is a bifurcation between the saturation and the stochastization of the magnetic island (appearance and disappearance of stochastization). A clear hysteresis in the relation between the size of the stochastic magnetic island and the magnetic shear is observed. This result suggests the importance of the magnetic shear to avoid the stochastic magnetic island at the rational surface.

We would like to thank the technical staff for their effort to support the experiment in LHD. This work is partly supported by a Grant-in-aid for Scientific research (No. 15206106) and the Grant-in-Aid for Specially-Promoted Research (No. 16002005) of MEXT Japan. This work is also partly supported by No. NIFS05LUBB510 and No. NIFS07KOAP017.

*Present address: Research Institute for Applied Mechanics, Kyushu University, Kasuga, Fukuoka 816-8580, Japan.

†Present address: Department of Quantum Science and Energy Engineering, Tohoku University, Sendai, Miyagi, 980-8679, Japan.

[1] Z. Chang *et al.*, Phys. Rev. Lett. **74**, 4663 (1995).
[2] O. Sauter *et al.*, Phys. Plasmas **4**, 1654 (1997).
[3] R. J. La Haye *et al.*, Nucl. Fusion **38**, 987 (1998).
[4] R. J. Buttery *et al.*, Phys. Rev. Lett. **88**, 125005 (2002).
[5] H. Zohm *et al.*, Phys. Plasmas **4**, 3433 (1997).
[6] A. Isayama *et al.*, Nucl. Fusion **43**, 1272 (2003).
[7] C. C. Petty *et al.*, Nucl. Fusion **44**, 243 (2004).
[8] K. Narihara *et al.*, Phys. Rev. Lett. **87**, 135002 (2001).
[9] N. Ohyabu *et al.*, Phys. Rev. Lett. **88**, 055005 (2002).
[10] K. Itoh *et al.*, Phys. Plasmas **12**, 072512 (2005).
[11] A. J. Lichtenberg *et al.*, Nucl. Fusion **32**, 495 (1992).
[12] A. Isayama *et al.*, Plasma Phys. Controlled Fusion **48**, L45 (2006).
[13] K. Ida *et al.*, Rev. Sci. Instrum. **76**, 053505 (2005).
[14] K. Kawahata *et al.*, Rev. Sci. Instrum. **74**, 1449 (2003).
[15] S. Inagaki *et al.*, Phys. Rev. Lett. **92**, 055002 (2004).
[16] W. A. Cooper, Plasma Phys. Controlled Fusion **34**, 1011 (1992).
[17] Y. Narushima *et al.*, J. Plasma Fusion Res. SERIES **6**, 214 (2004).
[18] S.-I. Itoh, K. Itoh, and M. Yagi, Plasma Phys. Controlled Fusion **46**, 123 (2004).
[19] T. S. Hahm *et al.*, Phys. Fluids **28**, 2412 (1985).
[20] A. H. Glasser *et al.*, Phys. Fluids **18**, 875 (1975).